Population Genomics Reveals Molecular Determinants of Specialization to Tomato in the Polyphagous Fungal Pathogen *Botrytis cinerea* in France

Alex Mercier[1,2], Adeline Simon[1], Nicolas Lapalu[1], Tatiana Giraud[3], Marc Bardin[4], Anne-Sophie Walker[1†], Muriel Viaud[1†] and Pierre Gladieux[5*†]

[1] Université Paris-Saclay, INRAE, AgroParisTech, UMR BIOGER, 78850 Thiverval-Grignon, France

[2] Université Paris-Saclay, Orsay, France

[3] Ecologie Systématique Evolution, CNRS, Université Paris-Saclay, AgroParisTech, 91400 Orsay, France

[4] UR0407 Pathologie Végétale, INRAE, 84143 Montfavet, France

[5] PHIM Plant Health Institute, Univ Montpellier, INRAE, CIRAD, Institut Agro, IRD, Montpellier, France

[*] Corresponding author: pierre.gladieux@inrae.fr

[†] contributed equally to this study

Abstract

Many fungal plant pathogens encompass multiple populations specialized on different plant species. Understanding the factors underlying pathogen adaptation to their hosts is a major challenge of evolutionary microbiology, and it should help preventing the emergence of new specialized pathogens on novel hosts. Previous studies have shown that French populations of the grey mould pathogen *Botrytis cinerea* parasitizing tomato and grapevine are differentiated from each other, and have higher aggressiveness on their host-of-origin than on other hosts, indicating some degree of host specialization in this polyphagous pathogen. Here, we aimed at identifying the genomic features underlying the specialization of *B. cinerea* populations to tomato and grapevine. Based on whole genome sequences of 32 isolates, we confirmed the subdivision of *B. cinerea* pathogens into two genetic clusters on grapevine and another, single cluster on tomato. Levels of genetic variation in the different clusters were similar, suggesting that the tomato-specific cluster has not recently emerged following a bottleneck. Using genome scans for selective sweeps and divergent selection, tests of positive selection based on polymorphism and divergence at synonymous and non-synonymous sites and analyses of presence/absence variation, we identified several candidate genes that represent possible determinants of host specialization in the tomato-associated population. This work deepens our understanding of the genomic changes underlying the specialization of fungal pathogen populations.

Keywords: Host specialization; grey mould; gene content variation; selective sweeps; positive selection

Introduction

Many fungal plant pathogens encompass multiple lineages, host races or *formae speciales* specialized on different plant species. Understanding the proximate (*i.e.* molecular) and ultimate (*i.e.* eco-evolutionary) factors underlying adaptation to hosts is a major goal for evolutionary microbiology, because emerging diseases are often caused by the appearance and spread of new pathogen populations specialized onto new hosts (Fisher *et al.* 2012; Stukenbrock & McDonald 2008). Evolutionary theory predicts that pathogen specialization should facilitate the emergence of new populations onto novel hosts, because specialization restricts encounters of potential mates within hosts and reduces the survival of offspring due to maladaptation of immigrants and hybrid offspring, thereby reducing gene flow between ancestral and emerging populations (Giraud *et al.* 2010; Nosil *et al.* 2005). The role of specialization as a barrier to gene flow is expected to be strong for pathogens mating within or onto their hosts because, for individuals evolving the ability to infect novel hosts, mating automatically becomes assortative with respect to host use, and reproductive isolation arises as a direct consequence of adaptive divergence (Gladieux *et al.* 2011; Servedio *et al.* 2011). Evolutionary theory also predicts that specialization, and the associated emergence of new populations, could be facilitated by the molecular basis of plant-pathogen interactions, because compatibility is often determined by a limited number of genes in the host and the pathogen, and selection is more efficient when it acts on a smaller number of genes (Giraud *et al.* 2010; Schulze-Lefert & Panstruga 2011). However, despite the apparent ubiquity of specialized fungal pathogens and the negative impact that specialized populations can have on food security and ecosystem health, the genomic features involved in host specialization

60 remain largely unknown. Acquiring knowledge about the genomic features underlying
61 pathogen specialization can provide key insights into the mechanisms of specialization.

62 The ascomycete *Botrytis cinerea* is often presented as a textbook example of a
63 polyphagous plant pathogen, parasitizing more than 1400 host plant species belonging to
64 580 genera (Elad *et al.* 2016). Previous population genetic studies reveal that *B. cinerea* is
65 not strictly speaking a generalist pathogen, and that a more appropriate qualifier is
66 "polyspecialist", i.e. a set of populations specialized to different host species. Indeed, with
67 the exception of California (Ma and Michailides, 2005; Caseys et al, 2020; Soltis et al, 2019;
68 Atwell et al, 2015), studies conducted in multiple regions of the world reveal that
69 populations were structured (reviewed in Walker 2016), and recognize the host as the factor
70 with the highest explanatory power for population structure in *B. cinerea*, ahead of
71 geography. In France, our previous work revealed population subdivision in *B. cinerea,* with
72 genetic differentiation between field populations infecting tomato (*Solanum lycopersicum*)
73 and grapevine (*Vitis vinifera*), respectively (Walker *et al.* 2015). This population structure in
74 *B. cinerea* was shown to be stable in time and was observed in multiple regions in France.
75 Furthermore, this structure was later associated with differences in performance on the two
76 hosts, with pathogens isolated from tomato being more aggressive on tomato than
77 pathogens isolated from grapevine, and reciprocally (Mercier *et al.* 2019). Altogether, these
78 data were consistent with a certain degree of specialization of *B. cinerea* populations onto
79 these two host plants.

80 Here, we aimed to identify the molecular basis of host specialization in the *B. cinerea*
81 tomato- and grapevine-associated populations, by addressing the following questions: (1)
82 Can we confirm the genetic subdivision between *B. cinerea* populations from tomato and

grapevine using genomic data, and what is the degree of divergence between them? (2) Can we identify genes with footprints of positive selection and/or divergent selection in the genomes of populations specialized to different hosts, and what are their predicted functions? (3) Is there variation in gene content between *B. cinerea* populations associated with tomato and grapevine? To address these questions, we used a set of *B. cinerea* isolates collected on tomato and grapevine in different regions of France. We Illumina-sequenced their genomes and identified single nucleotide polymorphisms by mapping sequencing reads against a high-quality reference genome (van Kan *et al.* 2017). Because some tests of selection can be biased by population subdivision, while other tests are based on patterns of population differentiation, we first analyzed the population structure of *B. cinerea* collected on tomato and grapevine. To detect genes potentially involved in the specialization of *B. cinerea* to tomato, we searched for signatures of positive selection, by scanning genomes in the tomato population for selective sweeps, and by estimating the direction and intensity of selection using McDonald-Kreitman tests on coding sequences. Furthermore, we investigated signatures of divergent selection using genomic differentiation between populations, and we characterized variations in the presence/absence of predicted genes between populations collected on tomato and grapevine using *de novo* genome assemblies, gene prediction, and orthology analysis.

102 ## Materials and methods

103 *Sample collection*

104 *Botrytis cinerea* samples were selected in a collection of isolates (i.e. single-spored mycelial
105 colonies) originating from three regions of France (Champagne, Occitanie and Provence) and
106 previously characterized using analyses of population structure based on microsatellite
107 markers and pathogenicity tests (Walker *et al.* 2015; Mercier *et al.*, 2019). For each region
108 and each host, we randomly selected three to nine isolates with high membership
109 proportions (q>0.9) in the cluster matching their host of origin in a previous analysis of
110 population structure based on microsatellite genotyping (Table 1; Mercier *et al.* 2019).
111 Collection sites were 15 to 133 km apart within regions, and 204 to 722 km apart between
112 regions (Supplementary Figure S1). The set of 32 isolates originated from the following
113 hosts: (i) tomato (*Solanum lycopersicum*; fruits; 13 isolates), (ii) grapevine (*Vitis vinifera*;
114 berries; 16 isolates), (iii) bramble (*Rubus fruticosus*; berries; two isolates) and (iv) hydrangea
115 (*Hydrangea macrophylla*; flower buds; one isolate). Samples from tomato originated from
116 plastic tunnels with sides opened (Occitanie region) or glasshouses (Provence and
117 Champagne regions). Mycelia were cultured on malt-yeast-agar (MYA; 20 $g.L^{-1}$ malt extract,
118 5 $g.L^{-1}$ yeast extract, 15 $g.L^{-1}$ agar) at 23°C under continuous light until conidiation, and
119 stored as conidial suspensions in glycerol 20% at -80°C until use.

120 *Pathogenicity tests on tomato plants*

121 Isolates of *B. cinerea* collected from tomato or grape were cultivated on MYA medium in a
122 growth chamber (21°C, 14 hours light) for 14 days. Conidia were then washed with sterile
123 distilled water. The conidial suspension was filtered through a 30 µm mesh sterile filter to

124 remove mycelium fragments. The conidial concentration was determined with a
125 haemacytometer and adjusted to 10^6 spores/mL. Seeds of tomato var. Clodano (Syngenta)
126 were sown in compost and transplanted after one week in individual pots. Plants were
127 grown in a glasshouse for 6 to 8 weeks where they received a standard commercial nutrient
128 solution once or twice a day, depending on needs. Plants had at least eight fully expanded
129 leaves when inoculated with a conidial suspension. Each isolate was inoculated on five
130 plants, from each of which two leaves were removed, leaving 5-10 mm petiole stubs on the
131 stems. Each pruning wound was inoculated with 10 µl of conidial suspension at 10^6
132 conidia/mL. Inoculated plants were incubated in a growth chamber in conditions conducive
133 to disease development (21°C, 16h-photoperiod, 162 $\mu mol.s^{-1}.m^{-2}$, relative humidity > 80%).
134 Due to a growth chamber area that did not allow all the isolates to be tested at the same
135 time, nine series of pathogenicity tests were conducted with 10-12 isolates each, together
136 with the BC1 reference isolate collected in 1989 in a tomato glasshouse in Brittany
137 (Decognet *et al.* 2009). For each isolate, two to four independent repetitions of the
138 pathogenicity test were performed. Lesion sizes (in mm) were assessed daily between the 4th
139 and the 7th day post-infection and the Area Under the Disease Progress Curve (AUDPC;
140 (Simko & Piepho 2012) was computed to take into account the kinetics of disease
141 development for each isolate. To compare the aggressiveness of isolates, an aggressiveness
142 index (AI), relative to the reference isolate BC1, was computed as follows: $AI_{isolate} =$
143 $100 \times (AUDPC_{isolate}/AUDPC_{BC1})$, where $AUDPC_{isolate}$ was the average AUDPC for a given
144 isolate and $AUDPC_{BC1}$ is the average AUDPC for the reference isolate BC1. Using the AI index
145 calibrating the AUDPC of a given isolate with that of the reference isolate BC1 in the same
146 test allows comparing isolates aggressiveness while taking into account the variability

occurring among assays (e.g. plant physiological state; (Leyronas *et al.* 2018). Because of data non-normality, data were analysed using non-parametric tests. Three statistical tests were carried out with STATISTICA: (1) we used a non-parametric analysis of variance (Kruskal-Wallis test) to assess differences among isolates in terms of aggressiveness on grape and tomato, considering the average values for each of the independent pathogenicity tests as replications; (2) we used the Mann-Whitney U-test to compare the aggressiveness of isolates from different hosts of origin (tomato vs. grape), considering the independent repetitions of the pathogenicity test as blocks and the 13 isolates from tomato and 16 isolates from grapevine as replicates; (3) we used a Kruskal-Wallis test to compare isolates from three different clusters (see *Results* section) in terms of aggressiveness on tomato plants.

DNA preparation and sequencing

Isolates were cultivated for 48 h on MYA + cellophane medium at 23 °C in the dark and then ground using a mortar and pestle in liquid nitrogen. DNA was extracted using a standard sarkosyl procedure (Dellaporta *et al.* 1983). Paired-end libraries were prepared and sequenced (2 x 100 nucleotides) on a HiSeq4000 Illumina platform at Integragen (Evry, France). Sequencing coverage ranged from 58 to 305 X. Genomic data were deposited at SRA under accession number PRJNA624742. Read quality was checked using FASTQC (https://www.bioinformatics.babraham.ac.uk/projects/fastqc/).

167 *SNP calling and filtering*

168 SNPs were detected with the same workflow as described in (Zhong *et al.* 2017). Sequencing
169 reads were preprocessed with TRIMMOMATIC v0.36 (Bolger *et al.* 2014). Preprocessed reads
170 were mapped onto the *B. cinerea* B05.10 reference genome (van Kan *et al.* 2017) using BWA
171 v0.7.15 (Li & Durbin 2009). Aligned reads were filtered based on quality using SAMTOOLS v1.3
172 (Li *et al.* 2009) and PICARD TOOLS (http://broadinstitute.github.io/picard/) to remove
173 secondary alignments, reads with a mapping quality <30 and paired reads not at the
174 expected distance. SNP calling was performed with FREEBAYES v1.1 (Garrison & Marth 2012).
175 Further filtering was carried out using script VCFFiltering.py
176 (https://urgi.versailles.inra.fr/download/gandalf/VCFtools-1.2.tar.gz), following (Li 2014).
177 We kept only biallelic SNPs supported by more than 90% of aligned reads, detected outside
178 low-complexity regions or transposable elements (as identified in the reference isolate
179 B05.10: https://doi.org/10.15454/TFYH9N; Porquier *et al.* 2016) and with coverage lower
180 than twice the standard deviation from the mean depth coverage. The VCF file is available
181 on Zenodo (doi: 10.5281/zenodo.4293375).

182

183 *Population structure and demographic history*

184 We performed a principal component analysis based on biallelic SNPs using the python
185 library SCIKIT-ALLEL 1.3.2 (https://github.com/cggh/scikit-allel). We used the sNMF program to
186 infer individual ancestry coefficients in *K* ancestral populations. This program is optimized for
187 the analysis of large datasets and it estimates individual admixture coefficients based on
188 sparse non-negative matrix factorization, without assuming Hardy-Weinberg equilibrium
189 (Frichot et al., 2014). We used SPLITSTREE 4 (Huson & Bryant 2005) to visualize relationships

190 between genotypes in a phylogenetic network, with reticulations representing the
191 conflicting phylogenetic signals caused by recombination or incomplete lineage sorting. The
192 position of the root was determined using a *B. fabae* isolate as the outgroup. *Botrytis fabae*
193 is one of the closest known relatives of *B. cinerea* (Amselem *et al.* 2011; Walker 2016).
194 Summary statistics of genomic variation (segregating sites S, nucleotide diversity π,
195 Watterson's θ, Tajima's D) were estimated using EGGLIB 3.0 (https://egglib.org/) on 10kb
196 windows, excluding sites with more than 50% missing data and removing windows with
197 lseff<1000 (lseff is the number of analysed sites) or nseff<3 (nseff is the average number of
198 exploitable samples). Site frequency spectra were estimated using DADI 1.7.0 (GUTENKUNST *ET*
199 *AL.* 2009). Allelic richness and private allele richness were estimated with ADZE 1.0 (Szpiech
200 *et al.* 2008), using a generalized rarefaction approach to account for differences in sample
201 size among populations.

202 We employed the f3 statistic (Reich *et al.* 2009) to test for admixture based on shared
203 genetic drift, as implemented in the POPSTATS python script (Skoglund *et al.* 2015;
204 https://github.com/pontussk/popstats/). The *f3* statistic is used to test for admixture among
205 three populations Px, P1, P2. In the no-admixture case, the *f3* statistic measures the branch
206 length between Px and the internal node of the unrooted population tree (Px;P1,P2), and it
207 is therefore expected to be greater than zero. In the case Px has a mixed ancestry from P1
208 and P2, or populations closely related to them, the *f3* statistic is expected to be negative.
209 Significance was assessed by block jackknife by treating each chromosome as a block and
210 weighting each block by the number of SNPs. The standard error of the test statistic was
211 used to define a Z-score.

212

213 *Genome assembly and gene prediction*

214 Gene content was determined using two independent approaches. In the first approach,
215 we used the read mapping coverage of the genes previously predicted in the reference
216 genome B05.10 (van Kan *et al.* 2017). Read count per site for each gene and for each isolate
217 was computed using SAMTOOLS BEDCOV, and normalized using EDGER (McCarthy *et al.* 2012;
218 Robinson *et al.* 2010). Genes showing significant differences in mapping coverage across
219 populations were identified with EDGER (adjusted p-value <0.05 and more than two-fold
220 change). Putative gene duplication events (higher mapping coverage) and missing B05.10
221 genes (lack of mapping reads) were visually inspected in their genomic context using a
222 genome browser for validation.

223 The second approach was based on genome assembly and *de novo* gene prediction.
224 Illumina paired-reads were assembled using a combination of VELVET (Zerbino & Birney
225 2008), SOAPDENOVO and SOAPGAPCLOSER (Luo *et al.* 2012), as follows: (1) reads were trimmed
226 at the first N, (2) contigs were generated with several k-mer values using SOAPDENOVO, (3)
227 several VELVET assemblies were built using several k-mer values and as the input the trimmed
228 reads and all SOAPDENOVO contigs considered as "long reads ", (4) the assembly that
229 maximizes the criterion (N50*size of the assembly) was selected, (5) SOAPGAPCLOSER was run
230 on the selected assembly, and (6) Contigs completely included in other longer contigs were
231 deleted. Genomic regions mapping to transposable elements previously identified in *B.*
232 *cinerea* (https://doi.org/10.15454/TFYH9N; Porquier *et al.* 2016) were masked with
233 REPEATMASKER (http://www.repeatmasker.org) prior to gene prediction. Genes were
234 predicted using the FGENESH *ab initio* gene-finder (Solovyev *et al.* 2006;

235 http://www.softberry.com/berry.phtml), the program previously used to annotate the
236 reference genome (Amselem *et al.* 2011), and for which *Botrytis*-specific gene-finding
237 parameters were thus available. Completeness of the assembly and gene prediction were
238 evaluated with BUSCO using the Ascomycota gene set (Seppey *et al.* 2019). We then used
239 ORTHOFINDER (Emms & Kelly 2015) in order to define groups of orthologous sequences
240 (hereafter "groups of orthologs") based on sequences of predicted genes translated into
241 protein sequences. To reduce the impact of incomplete gene prediction (*e.g.* truncated
242 genes in small contigs), groups of orthologs were then manually checked for the
243 presence/absence of the protein-encoding genes in the genomes using TBLASTN (Johnson *et*
244 *al.* 2008). Proteins were functionally annotated using INTERPROSCAN (Jones *et al.* 2014), and
245 SIGNALP (Almagro Armenteros *et al.* 2019) was used to predict secretion signal peptides.
246 Prediction of transmembrane helices in proteins was performed using TMHMM 2.0 (Krogh *et*
247 *al.* 2001; Sonnhammer *et al.*). As we detected traces of bacterial contamination in the
248 genome of the Sl13 isolate, this genome was not included in orthology analysis. However,
249 we have kept this genome for analyzes based on polymorphism, because bacterial reads
250 cannot map to the reference genome.
251

252 *Tests of positive selection based on polymorphism and divergence at synonymous and non-*
253 *synonymous sites*

254 We estimated the intensity and direction of selective pressures exerted on genes in
255 populations using the McDonald-Kreitman test based on polymorphism and divergence at
256 synonymous and non-synonymous sites (McDonald & Kreitman 1991). This test is based on
257 the number of nucleotide polymorphisms and substitutions in gene sequences, and assumes

258 that synonymous mutations are neutral. Pseudo-sequences for coding sequences of all
259 genes in the reference genome were generated using the VCF file and the reference
260 sequence. Synonymous and non-synonymous divergence was computed with CODEML (model
261 0; Yang 1997, 2007), using *B. fabae* as the outgroup. Synonymous and non-synonymous
262 polymorphism was computed using EGGLIB 3 (https://egglib.org/), filtering out sites with
263 more than 80% missing data and excluding filtered alignments with less than 10 codons or
264 four sequences. Samples Sl1, Sl2, Sl3, Sl13, Vv3, Vv5, Vv2, Vv4 and Vv6 were excluded
265 because they introduced missing data that prevented calculations of synonymous and non-
266 synonymous divergence. The neutrality index (NI), defined as $(P_N/D_N)/(P_S/D_S)$ (Stoletzki &
267 Eyre-Walker 2011), was computed for every gene, with P_N and D_N the numbers of non-
268 synonymous polymorphisms and substitutions, respectively, and P_S and D_S the numbers of
269 synonymous polymorphisms and substitutions, respectively. Pseudocounts of one were
270 added to each cell of the McDonald-Kreitman tables to ensure the NI was always defined
271 (*i.e.* no division by zero).
272
273 *Linkage disequilibrium and recombination*
274 We used POPLDDECAY (Zhang *et al.* 2019a) to measure linkage disequilibrium (r^2) as a function
275 of the distance between pairs of SNPs. POPLDDECAY was configured with a maximum distance
276 between SNPs of 300 kbp, a minor allele frequency of 0.005 and a maximum ratio of
277 heterozygous allele of 0.88. Recombination rates were estimated for each chromosome with
278 PAIRWISE in LDHAT version 2.2 (Auton & McVean 2007). Sites with missing data were excluded.
279
280 *Tests of positive selection based on linkage disequilibrium and the site frequency spectrum*

281 We searched for signatures of selective sweeps along genomes using three different
282 softwares, each implementing a different approach. The SWEED 3.0 software (Pavlidis *et al.*
283 2013) implements a composite likelihood ratio (*CLR*) test based on the SWEEPFINDER algorithm
284 (Nielsen *et al.* 2005), which uses the site frequency spectrum (SFS) of a locus to compute the
285 ratio of the likelihood of a hard selective sweep at a given position to the likelihood of a null
286 model hypothesis without selection. The CLR statistic was computed for each chromosomes
287 of each population using a grid size of 50 or 200 (grid size is the number of positions where
288 the likelihood is calculated), but only results for a grid size of 200 are presented because the
289 CLR profiles were highly similar between the two settings. Input files included both
290 "unfolded" SNPs (i.e. SNPs for which ancestral and derived states can be determined using
291 the allelic state of the outgroup) and "folded" SNPs (i.e. SNPs for which the outgroup had
292 missing data). Only biallelic sites with sample size greater than or equal to five were
293 included. The nS_L method implemented in the NSL software (Ferrer-Admetlla *et al.* 2014)
294 detects hard and soft selective sweeps based on haplotype homozygosity. The nSL statistic
295 was computed for each chromosome of each population, including only biallelic sites with
296 sample size greater than or equal to five. Nine isolates (Sl1, Sl2, Sl3, Sl13, Vv3, Vv5, Vv2, Vv4,
297 Vv6) were excluded to reduce the proportion of missing data. The *hapFLK* method (Fariello
298 *et al.* 2013) implemented in the HAPFLK software is based on the original *FLK* method by
299 (Bonhomme *et al.* 2010), which detects signatures of selection from differentiation between
300 populations. This metric was used to test the null hypothesis of neutrality by contrasting
301 allele frequencies at a given locus in different populations. *hapFLK* extends the FLK method
302 to account for the haplotype structure in the sample, and the method is robust to the effects
303 of bottlenecks and migration. HAPFLK takes the number of cluster of haplotypes as a

304 parameter (K). To determine the number of clusters of haplotypes K, we ran FASTPHASE v1.4
305 (Scheet & Stephens 2006) and R package IMPUTEQ (Khvorykh & Khrunin 2020) on
306 polymorphism data for the largest chromosome BCIN01. For each population, we used
307 IMPUTEQ to generate five datasets with 10% of polymorphic positions masked, and for each
308 masked dataset we used FASTPHASE for imputing masked positions assuming clusters of
309 K=2,3...10 haplotypes and the following parameters: -T10 -C25 -H-1 -n -Z. We estimated
310 error using Estimate-Errors function in IMPUTEQ and the number of clusters that minimizes
311 the error was selected as the optimum. The HapFLK metric was computed individually on
312 each chromosome using as number of clusters K = 5, and nfit = 2. Accessory chromosomes
313 were not included in these analyses as they showed presence/absence polymorphism (see
314 *Results* section).

315 **Results**

316 *Whole-genome sequencing, population structure and demographic history*

317 Previous work using microsatellite data revealed differentiation between populations of *B.*
318 *cinerea* collected on tomato and grapevine (Mercier *et al.* 2019; Walker *et al.* 2015). To
319 investigate the genetic basis of specialization of the tomato- and grapevine-infecting
320 populations, we randomly selected for genome sequencing 32 isolates collected on tomato
321 (13 isolates), grapevine (16 isolates), *Rubus* (two isolates) and *Hydrangea* (one isolate) (Table
322 1). Isolates from *Rubus* and *Hydrangea* were previously shown to belong to generalist
323 populations (*i.e.* assigned to clusters found on all sampled hosts; Mercier *et al.* 2019). One
324 isolate of the sister species *B. fabae* was also sequenced and used as the outgroup.
325 Information about the sequenced isolates is summarized in Table 1. Alignment of sequencing

326 reads to the B05.10 reference genome (van Kan *et al.* 2017) followed by SNP calling
327 identified 249,084 high-quality SNPs.

328 In clustering analyses based on sparse nonnegative matrix factorization algorithms, as
329 implemented in the sNMF program (Frichot et al., 2014), the model with *K*=4 clusters was
330 identified as the best model based on cross-entropy (Supplementary Figure S2) and models
331 with K>4 did not identify well-delimited and biologically relevant clusters (Fig. 1A). At K=4,
332 one cluster was associated with tomato (hereafter referred to as "T" cluster), two clusters
333 were associated with grapevine (hereafter referred to as "G1" for the largest, and "G2" for
334 the smallest), and one cluster was formed by the isolates Rf1 and Hm1 from bramble (*R.*
335 *fruticosus*) and hydrangea (*H. macrophylla*) (Figure 1A). The isolate Rf2 collected on wild
336 blackberry displayed ancestry in multiple clusters, and the reference isolate B05.10 had
337 ancestry in the G2 and T clusters. No pattern of geographical subdivision was observed,
338 consistent with previous findings (Walker *et al.* 2015; Mercier *et al.,* 2019). The neighbor-net
339 network inferred with SPLITSTREE revealed three main groups, corresponding to the three
340 main clusters identified with sNMF, with cluster G2 (isolates Vv8, Vv9, Vv11 and Vv15) more
341 closely related to T than to G1 (Figure 1B). Reticulations in the neighbor-net network and
342 patterns of membership at K=2 and K=3 in the analysis with sNMF indicated that cluster G2
343 shared recent ancestry with clusters G1 and T. However, tests for admixture using the f3
344 statistic (Reich *et al.* 2009; Skoglund *et al.* 2015) did not support a scenario in which G2
345 derived from admixture between the two other clusters (Supplementary Table S1). The
346 principal component analysis corroborated the results of clustering analyses and the
347 neighbor-net network (Figure 1C). The first principal component separated isolates Hm1 and
348 Rf1 from the rest of the dataset. The second principal component individualized isolate Rf2,

349 as well as the three clusters T, G1 and G2. The third and fourth principal components
350 individualized cluster G2 and isolate Sl11, respectively. Together, analyses of population
351 subdivision revealed three clearly defined populations (two on grapevine and one on
352 tomato) and we therefore focused on these populations to identify the genes underlying
353 differences in host specialization.

354 On average across core chromosomes BCIN01 to BCIN16, nucleotide diversity π and
355 Watterson's θ were comparable in the three populations (from π=0.0018/bp in G1 to π
356 =0.0030/bp in G2; from θ=0.0017/bp in G1 to θ=0.0027/bp in G2; Table 2; Supplementary
357 Table S2), although all comparisons were statistically significant except between populations
358 T and G2 for θ (two-tailed Wilcoxon signed-rank test, P-value>0.05). Allelic richness was
359 slightly higher in G2 than in T (AR=1.104 vs AR=1.094), and lower in G1 (AR=1.078). Private
360 allele richness was higher in G1 (PAR=0.085), than in T (PAR=0.073) and G2 (PAR=0.071)
361 (Table 2).

362 The site frequency spectra estimated in populations G1 and T were U-shaped, indicating
363 an excess of high-frequency derived alleles (Figure 2; population G2 was excluded because of
364 too small a sample size), consistent with ongoing episodes of positive selection, mis-
365 assignment of ancestral alleles or gene flow (Marchi & Excoffier 2020). Estimates of Tajima's
366 D were positive but close to zero in clusters T and G1 (T: D=0.309; G1: D=0.167), indicating a
367 slight deficit of low frequency variants (Table 2; Supplementary Table 2), consistent with
368 balancing selection or population contraction. In cluster G2, the estimated Tajima's D was
369 D=1.470 but the estimate was likely upwardly biased by the small sample size, because
370 Watterson's θ is underestimated when sample size is small. The distance at which linkage
371 disequilibrium (LD) decayed to 50% of its maximum was an order of magnitude longer in G2

372 (LDdecay50: 16,800bp) than in T (LDdecay50: 8600bp) and G1 (LDdecay50: 3100bp)
373 (Supplementary Figure S3). The recombination rate was higher in G2 (ρ=0.2047/bp) than in
374 G1 and T (G1: ρ=0.0178/bp; T: ρ=0.0108/bp).

375 The accessory chromosome BCIN18 showed no polymorphism in all three population and
376 the accessory chromosome BCIN17 showed no polymorphism in population G2
377 (Supplementary Table S2). However, it should be noted that coverage analysis also revealed
378 that these accessory chromosomes, which contain a reduced number of genes (23 and 19
379 respectively, van Kan *et al.* 2017), were distributed irrespectively of the host of origin:
380 BCIN17 was found present in all but three isolates (Sl9, Sl10 and Vv15), while BCIN18 was
381 only present in five isolates (Sl3, Sl5, Sl9, Vv9 and Vv11; Supplementary Table S3). In
382 population T, the accessory chromosome BCIN17 displayed a relatively high and positive
383 value of Tajima's D (D=1.37; Supplementary Table S2) and approximately twice as much
384 nucleotide diversity as in core chromosomes (π=0.0058/bp; Supplementary Table S2). In
385 population G1, accessory chromosome BCIN17 displayed a negative value of Tajima's D (D=-
386 0.845) and two orders of magnitude less nucleotide diversity than core chromosomes
387 (π=5.7e-5/bp; Supplementary Table S2). The differences in Tajima's D estimates for BCIN17
388 reflect the existence of two divergent haplotypes in T, but not in G1 (not shown).

389

390 *Isolates from the T population are more aggressive on tomato plants.*

391 To test whether isolates collected on tomato are more aggressive on their host of origin,
392 compared to isolates collected on grapevine, pathogenicity assays were performed on whole
393 tomato plants in controlled conditions. To assess differences among isolates in terms of
394 aggressiveness on grape and tomato, we used a non-parametric analysis of variance,

395 considering the average values for each of the independent pathogenicity tests as
396 replications. We found a significant isolate effect (Kruskal Wallis test, H (28, N= 87)
397 =69.89221, $p < 0.0001$), consistent with the wide range of aggressiveness levels observed for
398 the 29 isolates.

399 To compare the aggressiveness on tomato of isolates from different hosts of origin
400 (tomato vs. grape), we tested for differences in the distribution of the aggressiveness index
401 between isolates originating from the two types of hosts, considering the independent
402 repetitions of the pathogenicity test as blocks and the 13 isolates from tomato and 16
403 isolates from grapevine as replicates. We observed a significant effect of the host of origin
404 (Figure 3, Mann-Whitney U test, $p < 0.0001$) and T isolates collected on tomato were on
405 average 2.7 times more aggressive on tomato plants than isolates collected on grapevine.

406 To compare the aggressiveness on tomato of isolates from three different clusters (T, 13
407 isolates; G1, 12 isolates; G2, 4 isolates), we tested whether the aggressiveness index of
408 isolates from different clusters originate from the same distribution. A Kruskall-Wallis test
409 rejected the null hypothesis that all clusters display the same median of the aggressiveness
410 index (H (2, N= 87) =19.80083, $p < 0.0001$). The T population was significantly different from
411 the G1 population but not from G2 (Kruskall-Wallis test, $p< 0.0001$ and $p = 0.37$,
412 respectively). G2 and G1 were not significantly different (Kruskall-Wallis test, $p = 0.57$).

413

414 *Gene content slightly differs between tomato- and grapevine-associated populations*

415 As variation in gene content can be involved in adaptation to novel hosts (Cummings *et al.*
416 2004; Inoue *et al.* 2017; Langridge *et al.* 2015), we sought to identify genes specific to the
417 tomato (T) and grapevine (G1 and G2) populations. We first explored the mapping coverage

418 of genes previously identified in the B05.10 reference to identify sets of genes that were
419 missing or showing duplication events (Supplementary Table S4). Five B05.10 genes were
420 identified as missing in the T population, including four consecutive genes in the
421 subtelomeric region of chromosome BCIN02 that could correspond to a secondary
422 metabolism gene cluster. Among these four genes, one is coding for a NRPS-like enzyme
423 similar to the protein MelA of *Aspergillus terreus* involved in the biosynthesis of an α-keto
424 acid dimer (Geib et al. 2016), two other genes encode putative biosynthetic enzymes (FAD-
425 binding and enoyl reductase domains). Mapping coverage of B05.10 genes also suggested
426 some possible duplication events in a subtelomeric region of chromosome BCIN08, with T
427 isolates showing approximately three times as many reads as the G1 and G2 isolates for the
428 four consecutive genes Bcin08g00060 to Bcin08g00090. This suggested that the
429 corresponding region of at least 25 kb would be in three copies in the genomes of the T
430 isolates. Among the four duplicated genes, two encode carbohydrate-active enzymes
431 (CAZymes) known as plant cell wall degrading enzymes (PCWDEs) as they act on pectin
432 (glycoside hydrolase GH28) and hemicellulose or pectin side chains (GH43).

433 We also analysed the variation in gene content using a different approach that makes no
434 use of reference genome B05.10. We built *de novo* assemblies of the genomes of T, G1 and
435 G2 isolates. The genome assembly size of the 28 isolates ranged from 41 Mb to 42.5 Mb
436 (Supplementary Table S5), which was slightly smaller than the genome assembly size of the
437 B05.10 reference isolate (42.6 Mb). We then predicted genes *ab initio* using FGENESH. The
438 number of predicted genes ranged from 11,109 to 11,311 among genomes. To compare
439 gene content in the T, G1 and G2 populations, we used ORTHOFINDER to identify 12,319
440 groups of orthologous sequences (i.e., orthogroups). The number of groups of orthogroups

441 shared by pairs of isolates within populations was higher that between populations
442 (Supplementary Table S6). By looking for orthologous groups that were present in at least
443 75% of the genomes of a focal population and missing in other populations, we identified 21
444 G1-specific genes, a single G2-specific gene, five genes specific to the G1 and G2 populations
445 (those already detected with the first approach described above), two genes missing
446 specifically in the G1 population, and a single gene specific to the T population
447 (Supplementary Table S7). This latter gene was a GH71 glycoside hydrolase (OG0011490, an
448 α-1,3-glucanase; (Lombard *et al.* 2014) acting on fungal cell wall. Among the genes specific
449 to G1, we found a GH10 glycoside hydrolase (in OG0011469; (Lombard *et al.* 2014) acting on
450 plant cell wall (*i.e.* hemicellulose). The proteins encoded by the other G1-specific genes had
451 no functional prediction though four of them shared a domain typical of metalloenzymes
452 (IPR11249) with putative peptidase activities and three other ones showed a versatile
453 protein-protein interaction motif involved in many functions (IPR011333). Two proteins with
454 secretion signal peptides were also found specific to G1 (OG0011305 and OG0011366), with
455 OG0011366 having a predicted function of interferon alpha-inducible protein-like (Rosebeck
456 & Leaman 2008) and a predicted transmembrane helix.
457 Together, these analyses revealed that the magnitude of gene content variation is limited
458 between *B. cinerea* populations, which emphasizes the need to investigate differences in
459 allelic content at shared genes for elucidating the genomic basis of host specialization.
460

461 *McDonald-Kreitman tests of positive selection identify genes related to virulence*

462 We investigated differences in the direction and intensity of natural selection driving the
463 evolution of gene sequences in the two populations with the greatest difference in terms of

464 quantitative pathogenicity on grape and tomato, which are also the two populations with
465 the largest sample size (G1 and T). More specifically, we searched for genes with signatures
466 of positive selection in both populations that also show high sequence divergence between
467 populations, or genes with signatures of positive selection in one population, but not in the
468 other population. The direction and intensity of selection was estimated using neutrality
469 indexes computed for each individual gene in each population based on McDonald-Kreitman
470 tables of polymorphisms and substitutions at synonymous and non-synonymous sites, using
471 *B. fabae* as the outgroup. The neutrality index is expected to be below one for genes under
472 positive selection (due to an excess of non-synonymous substitutions) and above one for
473 genes under negative selection (due to a deficit of non-synonymous polymorphisms). To
474 identify genes potentially involved in host specialization, we first selected genes showing low
475 values of the neutrality index in both populations (log [neutrality index] ≤-0.5), and high
476 values of the inter-population dN/dS ratio (dN/dS in the top 5% percentile; Supplementary
477 Figure S4). This analysis identified five genes: Bcin02p04900, Bcin07p02650, Bcin09p06530,
478 Bcin14p01690, Bcin09p02190 (Supplementary Table S8). Two genes (Bcin07p02650,
479 Bcin14p01690) code for glycosyl hydrolases of the GH5 family, a family that includes
480 enzymes acting on plant cell walls and enzymes act on fungal cell walls. One of the two
481 genes (Bcin14p01690), has a cellulose binding domain which strongly suggests a role as
482 PCWDE. Two genes (Bcin02p04900, Bcin09p02190) are involved in basic cell functions (a
483 DNA nuclease and a protein involved in ribosome biogenesis). The last gene (Bcin09p06530)
484 has no known domain.

485 We also selected genes showing low values of the neutrality index in one population (log
486 [neutrality index] ≤-0.5), and high values in the other (log [neutrality index]>=0)

487 (Supplementary Figure S4). This analysis identified 392 genes in G1 and 428 genes in T
488 (Supplementary Table S8). Functional enrichment analyses revealed contrasting results in
489 the G1 and T populations (Supplementary Table S8). In the G1 population, we identified a
490 significant two-fold enrichment in transporter-encoding genes among the 392 genes with
491 signatures of positive selection. These 28 transporters included many candidates with
492 putative roles in nutrition such as the transport of sugars and amino-acids (five genes of
493 each). Fifteen of them were proteins of the major facilitator superfamily (MFS). The MFS
494 transporter-encoding genes included five putative sugar transporters and ten unknown
495 transporters that could have roles in various processes, including obtaining nutrients from
496 the host, efflux of fungi-toxic compounds or the export of fungal phytotoxins (Hartmann *et*
497 *al.* 2018; Maruthachalam *et al.* 2011; Perlin *et al.* 2014). Finally, five of the 392 genes
498 encoded ATPase transporters including the BcPrm1 P-type Ca2+/Mn2+-ATPase that
499 mediates cell-wall integrity and virulence in *B. cinerea* (Plaza *et al.* 2015).

500 In the T population, the list of 428 genes with signatures of positive selection showed a
501 significant 2.5-fold enrichment in genes encoding for proteins involved in oxidative stress
502 response (eight genes). These genes encode enzymes that are able to detoxify reactive
503 oxygen species *i.e.* glutathione-S-transferases (BcGST1, 9 and 24), the superoxide dismutase
504 BcSOD1, and two peroxidases (BcPRX8 and BcCCP1). In addition, the list of 428 genes also
505 included *BcatrO*, which encodes the transporter BcAtrO involved in the resistance to H_2O_2
506 (Pane *et al.* 2008).

507 A 2.5-fold enrichment was also observed for the genes coding for CAZYmes acting as
508 PCWDEs (ten genes) especially for those involved in the modification of hemicellulose (five

genes; Espino *et al.* 2010 ; Supplementary Table S8) such as the xylanase BcXyn11A that is required for full virulence on tomato (Brito *et al.* 2006).

Selective sweeps in regions encompassing genes encoding enzymes involved in carbohydrates metabolism

To identify genomic regions with signatures of selective sweeps, we conducted three different genome scans, using different features of the data: i) hapFLK, which detects hard and soft sweeps based on patterns of differentiation between clusters of haplotypes between populations; ii) nS_L, which detects hard and soft sweeps based on the distribution of fragment length between mutations and the distribution of the number of segregating sites between pairs of chromosomes; iii) and SweeD's CLR, which detects hard sweeps based on the site frequency spectrum. The *CLR* and nS_L metrics are population-specific and were computed for each population independently, while the *hapFLK* metric is F_{ST}-based and was thus computed for populations G1 and T (Supplementary figure S5). We identified candidate SNPs located in (hard or soft) selective sweeps as the SNPs that were in the top 5% of the hapFLK statistic, but also in the top 5% of either the nSL or CLR statistic in a least one population (Figure 4). In total, this approach identified 4,667 SNPs of which 1,300 were localized in coding sequences, 256 in introns, 830 in untranslated transcribed regions, and 465 less than 1500bp upstream of coding sequences. These 2,851 SNPs corresponded to 351 genes, of which 15 were identified by SNPs in the top 5% of selective sweep metrics in both populations, 200 by SNPs in the top 5% of selective sweep metrics in population T, and 175 by SNPs in the top 5% of selective sweep metrics in population G1 (Supplementary table S9).

531 Candidate genes in the selective sweep regions of each population included genes coding
532 for proteins with functions consistent with a role in infection, such as transporters, CAZymes,
533 putative effectors and two genes that are confirmed virulence factors. Indeed, one region
534 identified in the G1 population contains the gene encoding the Pectin Methyl Esterase
535 BcPme1 required for full virulence of *B. cinerea* on several host including grapevine (Valette-
536 Collet *et al.* 2003), and another region contains the gene encoding BcCgf1, a small secreted
537 protein that is essential for infection structure development (Zhang *et al.* 2020).
538 Nevertheless, it is unlikely that all genes in selective sweep regions have been direct targets
539 of positive selection, most of them being possible hitch-hikers. This could be the reason why
540 no significant functional enrichment was detected among these genes.
541 Finally, comparison of the lists of genes identified in the selective sweep regions and
542 those with signatures of positive selection according to McDonald-Kreitman tests identified
543 nine genes in common for the T population and four genes in common for the G1 population
544 (Supplementary table S9). This suggests that these genes were subjected to both recurrent
545 positive selection for amino-acid changes and to recent positive selection in populations of
546 *B. cinerea*. In addition, we can hypothesize that these genes may be the actual targets of
547 positive selection, and that surrounding candidate genes could be only hitch-hikers.
548 Functional annotations of the genes that show both recurrent positive selection for amino-
549 acid changes and recent positive selection signals further indicated a cutinase-encoding gene
550 (Bcin01g09430) in the T population and a sugar transporter encoding gene (Bcin16g00530) in
551 the G1 population, and also pointed out various other functions.
552

553 **Discussion**

554 *Genetic differentiation in* B. cinerea *between populations associated with grapevine and*
555 *tomato*

556 Genetic structure associated with the host of origin in *B. cinerea* has been extensively
557 investigated (reviewed in Walker 2016). Most of the studies based on sufficient sampling
558 size (n>100) found significant population differentiation between populations of *B. cinerea*
559 from different hosts (e.g. in Chile, Tunisia, Hungary, United Kingdom; Walker 2016). One
560 noticeable case is the population of *B. cinerea* collected from various hosts in California (Ma
561 & Michailides 2005), for which whole-genome sequencing data did not detect any host-
562 associated population structure despite differences in pathogenicity against different hosts
563 (including tomato) in cross-infectivity assays (Atwell *et al.* 2015; Caseys *et al.* 2020; Soltis *et*
564 *al.* 2019). In France, previous research concluded that *B. cinerea* populations were
565 differentiated according to some of their hosts, including tomato, grapevine and, to a lesser
566 extent, bramble (Fournier & Giraud 2008; Walker *et al.* 2015). In two recent studies
567 comparing the aggressiveness of isolates coming from diverse hosts, the disease severity
568 caused by isolates from tomato was significantly greater than the severity caused by isolates
569 from grape or other crops, thus indicating that *B. cinerea* populations parasitizing tomato
570 were specialized to this host (Bardin *et al.* 2018; Mercier *et al.* 2019). Here we show that
571 populations parasitizing tomato and grapevine are subdivided into three populations, two
572 being associated with grapevine (G1 and G2) and one with tomato (T). This pattern of
573 population genetic structure differs from previous findings (Walker et al., 2015), as three
574 populations parasitizing grapevine had previously been detected, but studies differ in terms
575 of sampling and genotyping schemes (thousands of SNPs vs 8 SSR markers, and an order of

576 magnitude of difference in the size of sample sets). The clear pattern of population
577 subdivision found in our study also stands in sharp contrast with the lack of host- or
578 geography-associated population subdivision across various hosts, including tomato and
579 grape, in California (Atwell *et al.* 2015; Atwell *et al.* 2018). This difference in population
580 structure between France and California indicates that the factors leading to host-specific
581 differentiation between *B. cinerea* pathogens from grape and tomato do not operate
582 everywhere. The differences in LD decay (up to an order of magnitude longer in our study
583 compared to Californian *B. cinerea*) and nucleotide diversity (half as much in our study
584 compared to Californian *B. cinerea*) also suggest that the demographic history and
585 population biology of the pathogen is contrasted between the two regions.

586 Multiple factors can contribute to reduce gene flow between populations parasitizing
587 grapevine and tomato. A first possible factor limiting gene flow is adaptation to host. Mating
588 in *B. cinerea* occurs on the host after infection, between individuals that were thus
589 sufficiently adapted to infect the same host, which induces assortative mating with respect
590 to host use and reduce opportunities for inter-population crosses (Giraud 2006; Giraud *et al.*
591 2010; Giraud *et al.* 2008). Another factor possibly limiting gene flow between populations
592 infecting tomato and grape is habitat isolation (*i.e.* reduced encounters caused by mating in
593 different habitats). Tomatoes are grown in nurseries before being dispatched to the fields,
594 tunnels or greenhouses, and this may generate habitat isolation if sexual reproduction in the
595 pathogen occurs in nurseries for the tomato-infecting population of *B. cinerea*. Such habitat
596 isolation may contribute to promote adaptation to tomato, by preventing the immigration of
597 alleles which are favorable for infection of non-tomato hosts but not favorable for infection
598 of tomato. Differences in the timing of epidemics are unlikely to contribute to this habitat

599 isolation, as the period of infection of greenhouse tomatoes runs from late to early winter,
600 which includes the period of infection of grape. The same goes for the location of epidemics,
601 since the sites studied were chosen because the two types of crops are grown nearby. A final
602 possibility to explain the lack of gene flow between *B. cinerea* populations from grape and
603 tomato is that the frequency of sexual reproduction might be lower in populations infecting
604 greenhouse tomatoes. Higher winter temperatures and the removal of plant residues in the
605 greenhouse represent conditions that are less conducive to sexual reproduction. However,
606 our estimates of LD decay and recombination rates are not consistent with a substantially
607 lower frequency of sexual reproduction in the population associated with tomato, compared
608 to the population associated with grape.

609 The differences in population structure observed between *B. cinerea* populations from
610 France and California could be due to different cultivation practices. In California, differences
611 in pathogenicity between tomato and other hosts did not lead to genome-wide
612 differentiation, indicating that gene flow occurs between hosts. In France, on the contrary,
613 differences in virulence are associated to genome-wide differentiation, indicating restriction
614 of gene flow. These differences in structure may be explained by the cultivation of tomatoes
615 in open fields in California, which favors dispersal to other crops, while French tomatoes are
616 generally grown in plastic tunnels or greenhouses.

617

618 *Widespread signatures of selection along genomes*

619 We identified little variation in the gene content among T, G1 and G2 populations, with one
620 gene specific to T, 22 genes specific to G1 and five genes shared between G1 and G2 but not
621 T, suggesting that gene gain or loss is not the main process of adaptation to tomato. In

622 parallel to our analysis of presence/absence variation, our genome scans for positive
623 selection pinpointed several genomic regions which may harbour determinants of ecological
624 differentiation between the population specialized to tomato and the population parasitizing
625 grapevine. In order to cover multiple time scales and different signatures of positive
626 selection, we used a variety of analytical approaches. The McDonald-Kreitman test focuses
627 on genes and detects repeated episodes of selective sweeps fixing non-synonymous
628 substitutions, thus generating a higher ratio of amino acid divergence to polymorphism (Dn /
629 Pn), relative to the ratio of silent divergence to polymorphism (Ds / Ps), than expected under
630 neutrality. The values of nucleotide diversity and Tajima's D measured in the T population
631 specialized in tomatoes were very close to the values measured for the two other
632 populations, which is not consistent with a very recent origin of this population and justifies
633 the use of the McDonald-Kreitman test. Genome scans for selective sweeps detect more
634 recent events, and by nature these methods can also detect genes that are not directly the
635 target of selection, but may have hitch-hiked due to physical linkage with sites under
636 positive selection. However, the LD decay values measured for the T population remain
637 moderate (9kb), and we used a combination of different selective sweep metrics to
638 substantially shorten the list of candidate genes, which should reduce the impact of genetic
639 hitch-hiking on our list of genes under recent positive selection. Despite using a more
640 conservative approach, we identified more selective sweeps than in the generalist
641 *Sclerotinia sclerotiorum* fungus (Derbyshire *et al.* 2019), or in the Californian generalist
642 population of *B. cinerea* (Soltis *et al.* 2019).
643

644 *Genes under positive selection*

645 We identified a number of genes showing signatures of positive selection using the
646 approaches discussed above and highlighting potential candidates for their role in host
647 specialization. Functional annotation of the *B. cinerea* genome and previous experimental
648 studies provided lists of genes involved in host-pathogen interaction and in other
649 developmental processes (Amselem *et al.* 2011; Nakajima & Akutsu 2014; Rodriguez-
650 Moreno *et al.* 2018). We used these published lists of genes to investigate whether some
651 specific biological processes were subjected to positive selection in the different
652 populations. Our data revealed that the five genes showing the strongest signatures of
653 selection in both the T and G1 populations, but also showing high sequence divergence
654 between the two populations, included two genes encoding for CAZymes with glycoside
655 hydrolase activity, which are potential PCWDEs. We also found that the 428 genes showing
656 the strongest signatures of selection in the T population with McDonald-Kreitman tests were
657 enriched both in genes coding for PCWDEs and in genes coding for enzymes involved in the
658 oxidative stress response. Notably, ten genes encoding secreted CAZymes targeting
659 compounds of the plant cell wall, *i.e.* cellulose and pectin (Amselem et al., 2011; Lombard *et*
660 *al.* 2014), were found under positive selection. One of these ten genes encodes the xylanase
661 BcXyn11A that has previously been shown to be a virulence factor on tomato (Brito *et al.*
662 2006). Another one encodes a cutinase (Bcin01g09430) that was further detected in a
663 selective sweep region suggesting, recurrent and recent positive selection events. Additional
664 PCWDEs were found in other genomic regions identified as selective sweeps. Finally, our
665 comparative genomic analysis suggested that a subtelomeric region that contains two
666 PCWDEs acting on pectin and/or hemicellulose is duplicated in the T population.

667 Necrotrophic species have important repertoires of CAZymes especially those corresponding
668 to PCWDEs which are known to act as major virulence factors in fungi (Zhao *et al.* 2013;
669 Rodriguez-Moreno *et al.* 2018). The genome of the reference isolate of *B. cinerea* (B05.10)
670 revealed 118 PCWDEs (Amselem et al., 2011) and our data suggest that, within this
671 repertoire, some cellulases and pectinases may be of particular importance for the
672 degradation of tomato cell wall. SNPs within a pectinesterase gene were also associated with
673 virulence on tomato in a previous genome-wide association study (Soltis *et al.* 2019).

674 In addition to PCWDEs, the single gene that was present in the T population but missing in
675 the G1 and G2 populations encoded a CAZyme acting on the fungal cell wall, an α-1,3-
676 glucanase classified as a member of the GH71 family. In the fungal cell wall, α-1,3-glucan is a
677 major component that encloses the α-(1,3)-glucan-chitin fibrillar core. Because of its
678 external localization and specific composition, α-1,3-glucan of pathogenic fungi plays a major
679 role in infection-related morphology and host recognition (Beauvais *et al.* 2013; King *et al.*
680 2017). A dozen of genes of *B. cinerea* encode for enzymes of the GH71 family (Amselem et
681 al., 2011). The T-specific GH71 CAZyme might therefore have been retained in the T
682 population as a mean to specifically facilitate infection of tomato by modification of the
683 fungal cell wall resulting in adaptive morphological changes or impairment of host
684 recognition.

685 As mentioned above, the McDonald-Kreitman tests also indicated that eight genes coding
686 for enzymes that detoxify reactive oxygen species showed signatures of positive selection in
687 the T population. During infection, *B. cinerea* encounters an oxidative burst, an early host
688 response that results in the death of plant cells. This mechanism is used in turn by *B. cinerea*
689 to achieve full virulence but this also implies that the fungus has to resist to this toxic

690 environment. The fungal oxidative stress response system includes detoxifying enzymes such
691 as superoxide dismutases (SODs) that convert O_2 into the less toxic H_2O_2, as well as
692 catalases, peroxidases and peroxiredoxins that convert H_2O_2. Additional non-enzymatic
693 mechanisms include the oxidation of compounds such as glutathione (Heller & Tudzynski
694 2011). In addition to the genes encoding SOD (BcSOD3), peroxidases (BcCCP1),
695 peroxiredoxins (BcPRX8) and other detoxifying enzymes sur as glutathione-S-transferases
696 (BcGST1, 9 and 24), a gene encoding the transporter BcAtrO also showed a signature of
697 positive selection in the T population. Inactivation of this gene previously suggested that it
698 allows the efflux of H_2O_2 and resistance this reactive oxygen species (Pane *et al.* 2008).
699 Altogether, our data suggest that the oxidative burst occurring in the *B. cinerea*/tomato
700 interaction is particularly challenging for the fungus.
701

702 *Concluding remarks*

703 We identified a population of *B. cinerea* specialized to tomato, which diverged from a
704 grapevine-associated population. Genome scans for selective sweeps and McDonald-
705 Kreitman tests revealed widespread signatures of positive selection that identified genes
706 that may contribute to the pathogen's adaptation to its tomato host. Candidate genes for
707 specialization to tomato were significantly enriched in those encoding cellulases, pectinases
708 and enzymes involved in the oxidative stress response, suggesting that the ability to degrade
709 the host cell wall and to cope with the oxidative burst are two key process in the *B.*
710 *cinerea*/tomato interaction. Our work sets the stage for future studies aiming to elucidate
711 the phenotypic and fitness effects of the candidate genes for specialization of *B. cinerea* to
712 tomato, for instance by knocking-out or replacing candidate genes for host specialization.

Acknowledgements

AM was supported by a grant from the Doctoral School « Sciences du Végétal », Université Paris-Saclay. We are grateful to INRAE-LIPM Bioinformatics Platform (Jérôme Gouzy, Sébastien Carrère, Erika Sallet, Ludovic Legrand) and Genotoul Bioinformatics Platforms Toulouse Occitanie (Bioinfo Genotoul, doi: 10.15454/1.5572369328961167E12) for providing computational support and resources. This work was supported by a grant overseen by the French National Research Agency (ANR) as part of the "Investissements d'Avenir" Programme (LabEx BASC; ANR-11-LABX-0034) and by the INRAE department SPE. The BIOGER unit also benefits from the support of "Saclay Plant Science-SPS" (ANR-17-EUR-0007).

725 ## References

726 Almagro Armenteros JJ, Tsirigos KD, Sonderby CK, *et al.* (2019) SignalP 5.0 improves signal peptide predictions
727 using deep neural networks. *Nature biotechnology* **37**, 420-423.
728 Amselem J, Cuomo CA, van Kan JA, *et al.* (2011) Genomic analysis of the necrotrophic fungal pathogens
729 *Sclerotinia sclerotiorum* and *Botrytis cinerea*. *PLoS genetics* **7**, e1002230.
730 Atwell S, Corwin J, Soltis N, *et al.* (2015) Whole genome resequencing of Botrytis cinerea isolates identifies high
731 levels of standing diversity. *Frontiers in microbiology* **6**, 996.
732 Atwell S, Corwin JA, Soltis N, *et al.* (2018) Resequencing and association mapping of the generalist pathogen
733 Botrytis cinerea. *bioRxiv*, 489799.
734 Auton A, McVean G (2007) Recombination rate estimation in the presence of hotspots. *Genome research* **17**,
735 1219-1227.
736 Bardin M, Leyronas C, Troulet C, Morris CE (2018) Striking similarities between Botrytis cinerea from non-
737 agricultural and from agricultural habitats. *Frontiers in plant science* **9**, 1820.
738 Beauvais A, Bozza S, Kniemeyer O, *et al.* (2013) Deletion of the α-(1,3)-glucan synthase genes induces a
739 restructuring of the conidial cell wall responsible for the avirulence of *Aspergillus fumigatus*. *PLoS*
740 *pathogens* **9**, e1003716.
741 Bolger AM, Lohse M, Usadel B (2014) Trimmomatic: a flexible trimmer for Illumina sequence data.
742 *Bioinformatics* **30**, 2114-2120.
743 Bonhomme M, Chevalet C, Servin B, *et al.* (2010) Detecting selection in population trees: the Lewontin and
744 Krakauer test extended. *Genetics* **186**, 241-262.
745 Brito N, Espino JJ, González C (2006) The endo-β-1, 4-xylanase Xyn11A is required for virulence in Botrytis
746 cinerea. *Molecular Plant-Microbe Interactions* **19**, 25-32.
747 Caseys C, Shi G, Soltis N, *et al.* (2020) Quantitative interactions drive *Botrytis cinerea* disease outcome across
748 the plant kingdom. *bioRxiv*, 507491.
749 Cummings CA, Brinig MM, Lepp PW, van de Pas S, Relman DA (2004) Bordetella species are distinguished by
750 patterns of substantial gene loss and host adaptation. *Journal of bacteriology* **186**, 1484-1492.
751 Decognet V, Bardin M, Trottin-Caudal Y, Nicot PC (2009) Rapid change in the genetic diversity of *Botrytis*
752 *cinerea* populations after the introduction of strains in a tomato glasshouse. *Phytopathology* **99**, 185-
753 193.
754 Dellaporta SL, Wood J, Hicks JB (1983) A plant DNA minipreparation: Version II. *Plant Molecular Biology*
755 *Reporter* **1**, 19-21.
756 Derbyshire MC, Denton-Giles M, Hane JK, *et al.* (2019) A whole genome scan of SNP data suggests a lack of
757 abundant hard selective sweeps in the genome of the broad host range plant pathogenic fungus
758 Sclerotinia sclerotiorum. *PloS one* **14**, e0214201.

759 Elad Y, Pertot I, Prado AMC, Stewart A (2016) Plant hosts of Botrytis spp. In: *Botrytis–the fungus, the pathogen*
760 *and its management in agricultural systems*, pp. 413-486. Springer.
761 Emms DM, Kelly S (2015) OrthoFinder: solving fundamental biases in whole genome comparisons dramatically
762 improves orthogroup inference accuracy. *Genome biology* **16**, 157.
763 Espino JJ, Gutierrez-Sanchez G, Brito N, *et al.* (2010) The *Botrytis cinerea* early secretome. *Proteomics* **10**, 3020-
764 3034.
765 Fariello MI, Boitard S, Naya H, SanCristobal M, Servin B (2013) Detecting signatures of selection through
766 haplotype differentiation among hierarchically structured populations. *Genetics* **193**, 929-941.
767 Ferrer-Admetlla A, Liang M, Korneliussen T, Nielsen R (2014) On detecting incomplete soft or hard selective
768 sweeps using haplotype structure. *Molecular biology and evolution* **31**, 1275-1291.
769 Fisher MC, Henk DlA, Briggs CJ, *et al.* (2012) Emerging fungal threats to animal, plant and ecosystem health.
770 *Nature* **484**, 186.
771 Fournier E, Giraud T (2008) Sympatric genetic differentiation of a generalist pathogenic fungus, *Botrytis cinerea,*
772 on two different host plants, grapevine and bramble. *Journal of Evolutionary Biology* **21**, 122-132.
773 Garrison E, Marth G (2012) Haplotype-based variant detection from short-read sequencing. *arXiv:1207.3907 [q-*
774 *bio].*
775 Geib E, Markus Gressler M, Iuliia Viediernikova I, Falk Hillmann F, Ilse D. Jacobsen ID, Sandor Nietzsche S,
776 Christian Hertweck C, Matthias Brock M (2016) A Non-canonical Melanin Biosynthesis Pathway
777 Protects Aspergillus terreus Conidia from Environmental Stress. *Cell Chemical Biology* **23**, 587-597.
778 Giraud T (2006) Speciation: Selection against migrant pathogens: the immigrant inviability barrier in pathogens.
779 *Heredity* **97**, 316-318.
780 Giraud T, Gladieux P, Gavrilets S (2010) Linking the emergence of fungal plant diseases with ecological
781 speciation. *Trends in ecology & evolution* **25**, 387-395.
782 Giraud T, Refrégier G, Le Gac M, de Vienne DM, Hood ME (2008) Speciation in fungi. *Fungal genetics and*
783 *biology : FG & B* **45**, 791-802.
784 Gladieux P, Guerin F, Giraud T, *et al.* (2011) Emergence of novel fungal pathogens by ecological speciation:
785 importance of the reduced viability of immigrants. *Molecular ecology* **20**, 4521-4532.
786 Gladieux P, Ravel S, Rieux A, *et al.* (2018) Coexistence of multiple endemic and pandemic lineages of the rice
787 blast pathogen. *MBio* **9**.
788 Gutenkunst RN, Hernandez RD, Williamson SH, Bustamante CD (2009) Inferring the joint demographic history
789 of multiple populations from multidimensional SNP frequency data. *PLoS genetics* **5**, e1000695.
790 Hartmann FE, McDonald BA, Croll D (2018) Genome-wide evidence for divergent selection between
791 populations of a major agricultural pathogen. *Molecular ecology* **27**, 2725-2741.
792 Heller J, Tudzynski P (2011) Reactive oxygen species in phytopathogenic fungi: signaling, development, and
793 disease. *Annual review of phytopathology* **49**, 369-390.
794 Huson DH, Bryant D (2005) Estimating phylogenetic trees and networks using SplitsTree 4. *Manuscript in*
795 *preparation, software available from www. splitstree. org.*

796 Inoue Y, Vy TTP, Yoshida K, *et al.* (2017) Evolution of the wheat blast fungus through functional losses in a host
797 specificity determinant. *Science* **357**, 80-83.
798 Johnson M, Zaretskaya I, Raytselis Y, *et al.* (2008) NCBI BLAST: a better web interface. *Nucleic acids research* **36**,
799 W5-W9.
800 Jones P, Binns D, Chang HY, *et al.* (2014) InterProScan 5: genome-scale protein function classification.
801 *Bioinformatics* **30**, 1236-1240.
802 Khvorykh GV, Khrunin AV (2020) imputeqc: an R package for assessing imputation quality of genotypes and
803 optimizing imputation parameters. *BMC bioinformatics* **21**, 1-14.
804 King R, Urban M, Lauder RP, *et al.* (2017) A conserved fungal glycosyltransferase facilitates pathogenesis of
805 plants by enabling hyphal growth on solid surfaces. *PLoS pathogens* **13**, e1006672.
806 Krogh A, Larsson B, Von Heijne G, Sonnhammer ELL (2001) Predicting transmembrane protein topology with a
807 hidden Markov model: application to complete genomes. *Journal of molecular biology* **305**, 567-580.
808 Langridge GC, Fookes M, Connor TR, *et al.* (2015) Patterns of genome evolution that have accompanied host
809 adaptation in *Salmonella*. *Proceedings of the National Academy of Sciences of the United States of*
810 *America* **112**, 863-868.
811 Leyronas C, Bardin M, Berthier K, *et al.* (2018) Assessing the phenotypic and genotypic diversity of *Sclerotinia*
812 *sclerotiorum* in France. *European journal of plant pathology* **152**, 933-944.
813 Li H (2014) Toward better understanding of artifacts in variant calling from high-coverage samples.
814 *Bioinformatics (Oxford, England)* **30**, 2843-2851.
815 Li H, Durbin R (2009) Fast and accurate short read alignment with Burrows-Wheeler transform. *Bioinformatics*
816 **25**, 1754-1760.
817 Li H, Handsaker B, Wysoker A, *et al.* (2009) The Sequence Alignment/Map format and SAMtools. *Bioinformatics*
818 **25**, 2078-2079.
819 Lombard V, Golaconda Ramulu H, Drula E, Coutinho PM, Henrissat B (2014) The Carbohydrate-Active enZymes
820 database (CAZy) in 2013. *Nucleic acids research* **42**, D490-495.
821 Luo R, Liu B, Xie Y, *et al.* (2012) SOAPdenovo2: an empirically improved memory-efficient short-read de novo
822 assembler. *GigaScience* **1**, 18.
823 Ma Z, Michailides TJ (2005) Genetic structure of Botrytis cinerea populations from different host plants in
824 California. *Plant disease* **89**, 1083-1089.
825 Marchi N, Excoffier L (2020) Gene flow as a simple cause for an excess of high-frequency-derived alleles.
826 *Evolutionary applications* **13**, 2254-2263.
827 Maruthachalam K, Klosterman SJ, Kang S, Hayes RJ, Subbarao KV (2011) Identification of pathogenicity-related
828 genes in the vascular wilt fungus *Verticillium dahliae* by *Agrobacterium tumefaciens*-mediated T-DNA
829 insertional mutagenesis. *Molecular Biotechnology* **49**, 209-221.
830 McCarthy DJ, Chen Y, Smyth GK (2012) Differential expression analysis of multifactor RNA-Seq experiments
831 with respect to biological variation. *Nucleic acids research* **40**, 4288-4297.

832 McDonald JH, Kreitman M (1991) Adaptive protein evolution at the Adh locus in *Drosophila*. *Nature* **351**, 652-
833 654.
834 Mercier A, Carpentier F, Duplaix C*, et al.* (2019) The polyphagous plant pathogenic fungus *Botrytis cinerea*
835 encompasses host-specialized and generalist populations. *Environmental microbiology*.
836 Nakajima M, Akutsu K (2014) Virulence factors of *Botrytis cinerea*. *Journal of General Plant Pathology* **80**, 15-23.
837 Nielsen R, Beaumont MA (2009) Statistical inferences in phylogeography. *Molecular ecology* **18**, 1034-1047.
838 Nielsen R, Williamson S, Kim Y*, et al.* (2005) Genomic scans for selective sweeps using SNP data. *Genome*
839 *research* **15**, 1566-1575.
840 Nosil P, Vines TH, Funk DJ (2005) Perspective: reproductive isolation caused by natural selection against
841 immigrants from divergent habitats. *Evolution; international journal of organic evolution* **59**, 705-719.
842 Pane C, Rekab D, Firrao G, Ruocco M, Scala F (2008) A NOVEL GENE CODING FOR AN ABC TRANSPORTER IN
843 BOTRYTIS CINEREA (BOTRYOTINIA FUCKELIANA) IS INVOLVED IN RESISTANCE TO H^+ O^+. *Journal of*
844 *Plant Pathology*, 453-462.
845 Pavlidis P, Zivkovic D, Stamatakis A, Alachiotis N (2013) SweeD: likelihood-based detection of selective sweeps
846 in thousands of genomes. *Molecular biology and evolution* **30**, 2224-2234.
847 Perlin MH, Andrews J, Toh SS (2014) Essential letters in the fungal alphabet: ABC and MFS transporters and
848 their roles in survival and pathogenicity. *Advances in genetics* **85**, 201-253.
849 Plaza V, Lagües Y, Carvajal M*, et al.* (2015) bcpmr1 encodes a P-type Ca2+/Mn2+-ATPase mediating cell-wall
850 integrity and virulence in the phytopathogen Botrytis cinerea. *Fungal Genetics and Biology* **76**, 36-46.
851 Porquier A, Morgant G, Moraga J*, et al.* (2016) The botrydial biosynthetic gene cluster of *Botrytis cinerea*
852 displays a bipartite genomic structure and is positively regulated by the putative Zn(II)2Cys6
853 transcription factor BcBot6. *Fungal genetics and biology : FG & B* **96**, 33-46.
854 Reich D, Thangaraj K, Patterson N, Price AL, Singh L (2009) Reconstructing Indian population history. *Nature*
855 **461**, 489-494.
856 Robinson MD, McCarthy DJ, Smyth GK (2010) edgeR: a Bioconductor package for differential expression
857 analysis of digital gene expression data. *Bioinformatics (Oxford, England)* **26**, 139-140.
858 Rodriguez-Moreno L, Ebert MK, Bolton MD, Thomma BPHJ (2018) Tools of the crook- infection strategies of
859 fungal plant pathogens. *The Plant journal : for cell and molecular biology* **93**, 664-674.
860 Rosebeck S, Leaman DW (2008) Mitochondrial localization and pro-apoptotic effects of the interferon-inducible
861 protein ISG12a. *Apoptosis : an international journal on programmed cell death* **13**, 562-572.
862 Scheet P, Stephens M (2006) A fast and flexible statistical model for large-scale population genotype data:
863 applications to inferring missing genotypes and haplotypic phase. *The American Journal of Human*
864 *Genetics* **78**, 629-644.
865 Schulze-Lefert P, Panstruga R (2011) A molecular evolutionary concept connecting nonhost resistance,
866 pathogen host range, and pathogen speciation. *Trends in plant science* **16**, 117-125.
867 Seppey M, Manni M, Zdobnov EM (2019) BUSCO: assessing genome assembly and annotation completeness.
868 In: *Gene Prediction*, pp. 227-245. Springer.

869 Servedio MR, Van Doorn GS, Kopp M, Frame AM, Nosil P (2011) Magic traits in speciation: 'magic' but not rare?
870 *Trends in ecology & evolution* **26**, 389-397.
871 Simko I, Piepho H-P (2012) The area under the disease progress stairs: calculation, advantage, and application.
872 *Phytopathology* **102**, 381-389.
873 Skoglund P, Mallick S, Bortolini MC, *et al.* (2015) Genetic evidence for two founding populations of the
874 Americas. *Nature* **525**, 104-108.
875 Solovyev V, Kosarev P, Seledsov I, Vorobyev D (2006) Automatic annotation of eukaryotic genes, pseudogenes
876 and promoters. *Genome biology* **7**, S10.11-12.
877 Soltis NE, Atwell S, Shi G, *et al.* (2019) Interactions of tomato and Botrytis cinerea genetic diversity: Parsing the
878 contributions of host differentiation, domestication, and pathogen variation. *The Plant Cell* **31**, 502-
879 519.
880 Sonnhammer ELL, Von Heijne G, Krogh A A hidden Markov model for predicting transmembrane helices in
881 protein sequences **6**, 175-182.
882 Stoletzki N, Eyre-Walker A (2011) Estimation of the neutrality index. *Molecular biology and evolution* **28**, 63-70.
883 Stukenbrock EH, McDonald BA (2008) The origins of plant pathogens in agro-ecosystems. *Annual review of*
884 *phytopathology* **46**, 75-100.
885 Szpiech ZA, Jakobsson M, Rosenberg NA (2008) ADZE: a rarefaction approach for counting alleles private to
886 combinations of populations. *Bioinformatics (Oxford, England)* **24**, 2498-2504.
887 Valette-Collet O, Cimerman A, Reignault P, Levis C, Boccara M (2003) Disruption of Botrytis cinerea pectin
888 methylesterase gene Bcpme1 reduces virulence on several host plants. *Molecular Plant-Microbe*
889 *Interactions* **16**, 360-367.
890 van Kan JA, Stassen JH, Mosbach A, *et al.* (2017) A gapless genome sequence of the fungus *Botrytis cinerea*.
891 *Molecular plant pathology* **18**, 75-89.
892 Walker A (2016) Diversity within and between species of *Botrytis*. In: *Botrytis - The Fungus, the Pathogen and*
893 *its Management in Agricultural Systems* (eds. Fillinger S, Elad Y), pp. 91-125.
894 Walker A, Gladieux P, Decognet V, *et al.* (2015) Population structure and temporal maintenance of the
895 multihost fungal pathogen *Botrytis cinerea*: causes and implications for disease management.
896 *Environmental microbiology* **17**, 1261-1274.
897 Yang Z (1997) PAML: a program package for phylogenetic analysis by maximum likelihood. *Computer*
898 *applications in the biosciences* **13**, 555-556.
899 Yang Z (2007) PAML 4: phylogenetic analysis by maximum likelihood. *Molecular biology and evolution* **24**, 1586-
900 1591.
901 Zerbino DR, Birney E (2008) Velvet: algorithms for de novo short read assembly using de Bruijn graphs. *Genome*
902 *research* **18**, 821-829.
903 Zhang C, Dong SS, Xu JY, He WM, Yang TL (2019a) PopLDdecay: a fast and effective tool for linkage
904 disequilibrium decay analysis based on variant call format files. *Bioinformatics (Oxford, England)* **35**,
905 1786-1788.

906 Zhang C, Dong SS, Xu JY, He WM, Yang TL (2019b) PopLDdecay: a fast and effective tool for linkage
907 disequilibrium decay analysis based on variant call format files. *Bioinformatics* **35**, 1786-1788.
908 Zhang MZ, Sun CH, Liu Y, *et al.* (2020) Transcriptome analysis and functional validation reveal a novel gene,
909 BcCGF1, that enhances fungal virulence by promoting infection-related development and host
910 penetration. *Molecular plant pathology* **21**, 834-853.
911 Zhao Z, Liu H, Wang C, Xu JR (2013) Comparative analysis of fungal genomes reveals different plant cell wall
912 degrading capacity in fungi. *BMC genomics* **14**, 274.
913 Zhong Z, Marcel TC, Hartmann FE, *et al.* (2017) A small secreted protein in *Zymoseptoria tritici* is responsible for
914 avirulence on wheat cultivars carrying the Stb6 resistance gene. *The New phytologist* **214**, 619-631.
915

Table 1. *Botrytis* isolates included in the study. Isolates from grapevine berries and tomatoes were collected in three regions of France between September 2005 and June 2007 for Champagne and Provence isolates (Walker *et al.* (2015), and between May and June 2009 for Occitanie isolates. Tomatoes in Occitanie were grown in plastic tunnels with sides open, whereas those from the Champagne and Provence areas were grown in glass-greenhouses. B05.10 is used as the reference isolate for genomic analysis (van Kan et al. 2016)

Species	Isolate ID	Other ID	Host, cultivar	Region, city
B. cinerea	Vv1	VC636	*Vitis vinifera,* Pinot noir	Champagne, Hautvilliers
	Vv2	VC095	*Vitis vinifera,* Pinot noir	Champagne, Vandières
	Vv3	VC621	*Vitis vinifera,* Pinot noir	Champagne, Hautvilliers
	Vv4	VC671	*Vitis vinifera,* Pinot noir	Champagne, Hautvilliers
	Vv5	VC224	*Vitis vinifera,* Pinot meunier	Champagne, Courteron
	Vv6	VC624	*Vitis vinifera,* Pinot noir	Champagne, Hautvilliers
	Vv7	ACBER342	*Vitis vinifera,* Grenache	Provence, Berre
	Vv8	ACBER356	*Vitis vinifera,* Grenache	Provence, Berre
	Vv9	ACBER358	*Vitis vinifera,* Grenache	Provence, Berre
	Vv10	ACSAR333	*Vitis vinifera,* Grenache	Provence, Sarrians
	Vv11	ACSAR334	*Vitis vinifera,* Grenache	Provence, Sarrians
	Vv12	ACSAR335	*Vitis vinifera,* Grenache	Provence, Sarrians
	Vv13	ACSAR342	*Vitis vinifera,* Grenache	Provence, Sarrians
	Vv14	ACSAR354	*Vitis vinifera,* Grenache	Provence, Sarrians
	Vv15	ACSAR357	*Vitis vinifera,* Grenache	Provence, Sarrians
	Vv16	VC610	*Vitis vinifera,* Pinot noir	Champagne, Hautvilliers
	Sl1	VA714	*Solanum lycopersicum,* Moneymaker	Champagne, Foissy-sur-Vanne
	Sl2	VC800	*Solanum lycopersicum,* Moneymaker	Champagne, Courceroy
	Sl3	VC806	*Solanum lycopersicum,* Moneymaker	Champagne, Courceroy
	Sl4	AABER19	*Solanum lycopersicum*, Alison	Provence, Berre
	Sl5	ACBER304	*Solanum lycopersicum*, Alison	Provence, Berre
	Sl6	ACPIE306	*Solanum lycopersicum,* Hipop	Provence, Pierrelatte
	Sl7	ADPIE463	*Solanum lycopersicum,* Hipop	Provence, Pierrelatte
	Sl8	ADPIE475	*Solanum lycopersicum,* Hipop	Provence, Pierrelatte
	Sl9	65_TT8	*Solanum lycopersicum*, Brenda	Occitanie, Alenya
	Sl10	5_TT8	*Solanum lycopersicum*, Brenda	Occitanie, Alenya
	Sl11	13_TT8	*Solanum lycopersicum*, Brenda	Occitanie, Alenya

	Sl12	9_TT8	*Solanum lycopersicum*, Brenda	Occitanie, Alenya
	Sl13	66_TT8	*Solanum lycopersicum*, Brenda	Occitanie, Alenya
	Rf1	VC902	*Rubus fruticosus*, wild	Champagne, Foissy-sur-Vanne
	Rf2	VC399	*Rubus fruticosus*, wild	Champagne, Courteron
	Hm1	MSN-Bot 2556	*Hydrangea macrophylla*, Leuchtfeuer	Anjou, Angers
	B05.10	-	-	-
B. fabae	Bfab	MSN-Bot 2220	*Vicia faba*	Region of Tunis (Tunisia)

Table 2. Summary statistics of genomic variation in three clusters of *Botrytis cinerea*

Cluster	S	π	θ	AR	PAR	D	H	LD50	ρ
T	37763	0.0027	0.0026	1.094 (0.0002)	0.073 (0.0002)	0.309	0.451	8600	0.0108
G1	26769	0.0018	0.0017	1.078 (0.0002)	0.085 (0.0002)	0.167	0.230	3100	0.0178
G2	14307	0.0030	0.0027	1.104 (0.0003)	0.071 (0.0002)	1.470	0.140	16800	0.2047

S, number of segregating sites; π, nucleotide diversity per site; θ, Watterson's estimate of the population mutation parameter per site; ρ, population recombination parameter per site; AR, allelic richness (standard error of the mean); PAR, private allele richness (standard error of the mean); D, Tajima's D; H, Fay and Wu's standardised H; LD50, distance (in bp) at which linkage disequilibrium reaches half of its maximum value. Only core chromosomes BCIN01 to BCIN16 were included in calculations. Per site estimates of π, ρ and θ were computed by summing across chromosomes and dividing by number of sites covered. Tajima's D and Fay and Wu's standardised H were computed across 10kb windows, and averaged. AR and PAR were computed using a generalized rarefaction approach and a standardized sample size of two haploid genomes.

Figure Captions

Figure 1. Population subdivision inferred based on SNPs identified in 32 isolates of *Botrytis cinerea* collected on tomato (red, Sl prefix, *Solanum lycopersicum*), grape (green, Vv prefix, *Vitis vinifera*), bramble (black, Rf prefix, *Rubus fruticosus*) and hydrangea (black, Hm prefix, *Hydrangea macrophylla*). (A) Ancestry proportions in K clusters, as estimated with the sNMF program. Each multilocus genotype is represented by a vertical bar divided into K segments, indicating membership in K clusters. (B) Neighbor-net phylogenetic network estimated with SPLITSTREE, with one isolate of *B. fabae* (Bfab) used as the outgroup. Reticulations indicate phylogenetic conflicts caused by recombination or incomplete lineage sorting. (C) Principal component analysis showing first four principal components PC1, PC2, PC3 and PC4. Isolate B05.10 in (A) and (B) is the reference genome for *B. cinerea* (van Kan et al. 2016)

Figure 2. Site frequency spectra estimated in populations T2 and Vv1 based on 85,415 SNPs using the python package DADI, projecting sample sizes to seven haploid genomes. Projection consists in averaging over all possible re-samplings of the larger sample size data, thus biallelic positions with data for less than seven individuals are not included in calculations and not counted as SNPs.

Figure 3. Boxplots representing the extent of aggressiveness (% relative to the reference isolate BC1) on tomato of the *Botrytis cinerea* isolates collected on grapevine (n=16) and tomato (n=13). For each boxplot, mean (crosses), median (horizontal lines), values of the aggressiveness index (circles), 25-75% quartiles, and maximum and minimum values are represented.

Figure 4. Genome scans for selective sweeps in the T and G1 populations of *Botrytis cinerea*, parasitizing tomato and grapevine, respectively. (A) and (C): Composite likelihood ratio

(CLR) estimated using the SWEED software (Nielsen *et al.* 2005; Pavlidis *et al.*, 2013) in T and G1, respectively. (B) and (D) Number of segregating sites by length, nS_L, estimated using the NSL software (Ferrer-Admetlla *et al.* 2014) in T and G1, respectively. (E) hapFLK statistic estimated using the HAPFLK software (Bonhomme *et al.* 2010; Fariello *et al.* 2013). Horizontal dashed black lines represent the top 5%. Vertical dashed grey lines represent the boundaries of the 16 chromosomes and the chromosome names are set along the x axis. SNPs in chromosomes with names ending with odd numbers are represented in dark colors, while SNPs in chromosomes with names ending with even numbers are represented in light colors. Black dots represent SNPs belonging to the following set: [(top 5% CLR population G1) ∪ (top 5% CLR population T) ∪ (top 5% nSL population G1) ∪ (top 5% nSL population T)] ∩ [top 5% hapFLK].

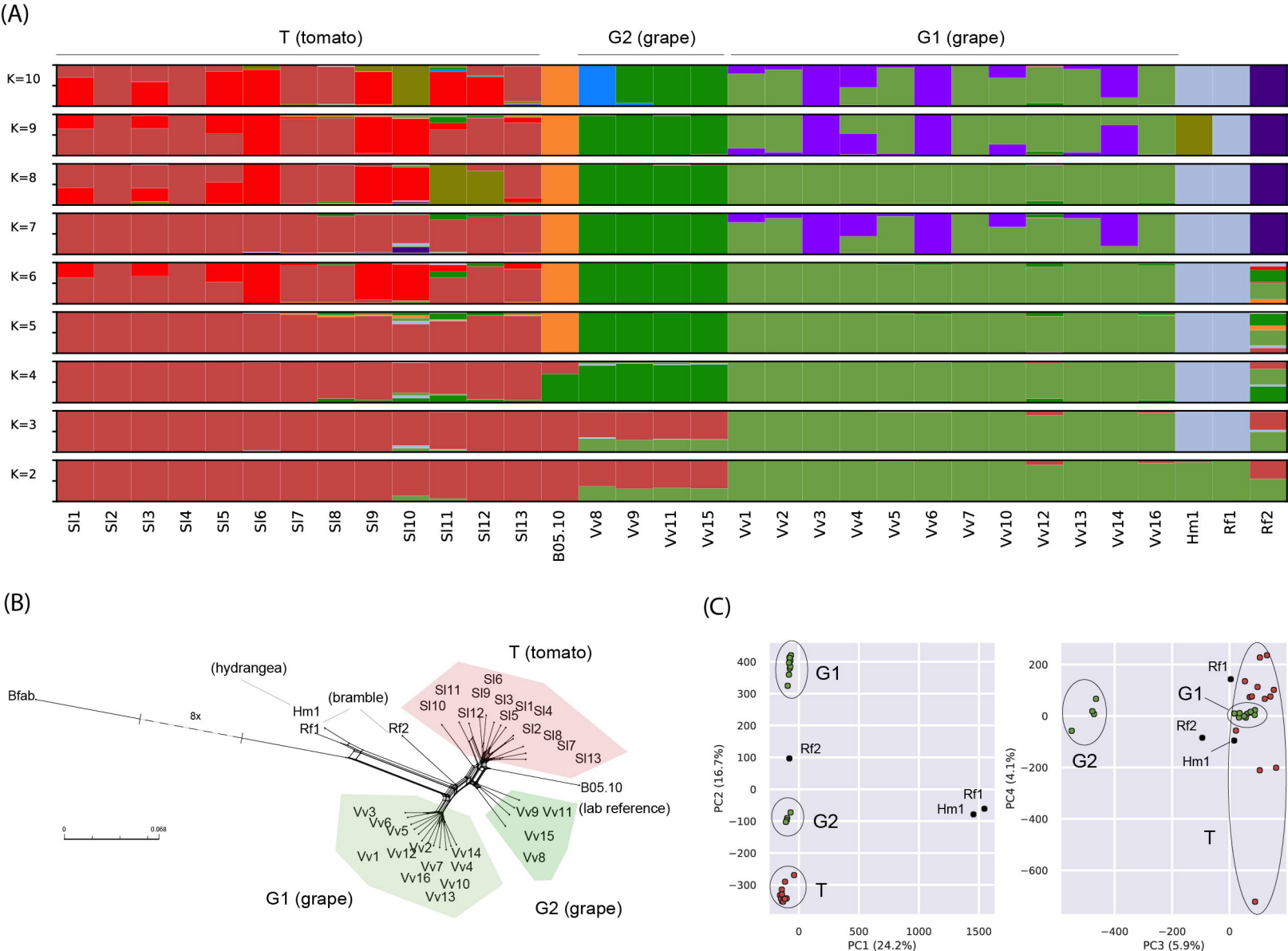
(A)
T (tomato)
G2 (grape)
G1 (grape)
K=10
K=9
K=8
K=7
K=6
K=5
K=4
K=3
K=2
Sl1 Sl2 Sl3 Sl4 Sl5 Sl6 Sl7 Sl8 Sl9 Sl10 Sl11 Sl12 Sl13 B05.10 Vv8 Vv9 Vv11 Vv15 Vv1 Vv2 Vv3 Vv4 Vv5 Vv6 Vv7 Vv10 Vv12 Vv13 Vv14 Vv16 Hm1 Rf1 Rf2
(B)
T (tomato)
(hydrangea)
Bfab
8x
Hm1
(bramble)
Rf1
Rf2
Sl6
Sl11
Sl9
Sl3
Sl1
Sl4
Sl10
Sl12
Sl5
Sl2
Sl8
Sl7
Sl13
B05.10
(lab reference)
Vv9 Vv11
Vv15
Vv8
Vv3
Vv6
Vv5
Vv1
Vv12
Vv2
Vv14
Vv7
Vv4
Vv16
Vv10
Vv13
0
0.068
G1 (grape)
G2 (grape)
(C)
G1
Rf2
G2
Rf1
Hm1
T
PC2 (16.7%)
PC1 (24.2%)
PC4 (4.1%)
PC3 (5.9%)
G2
Rf1
G1
Rf2
Hm1
T

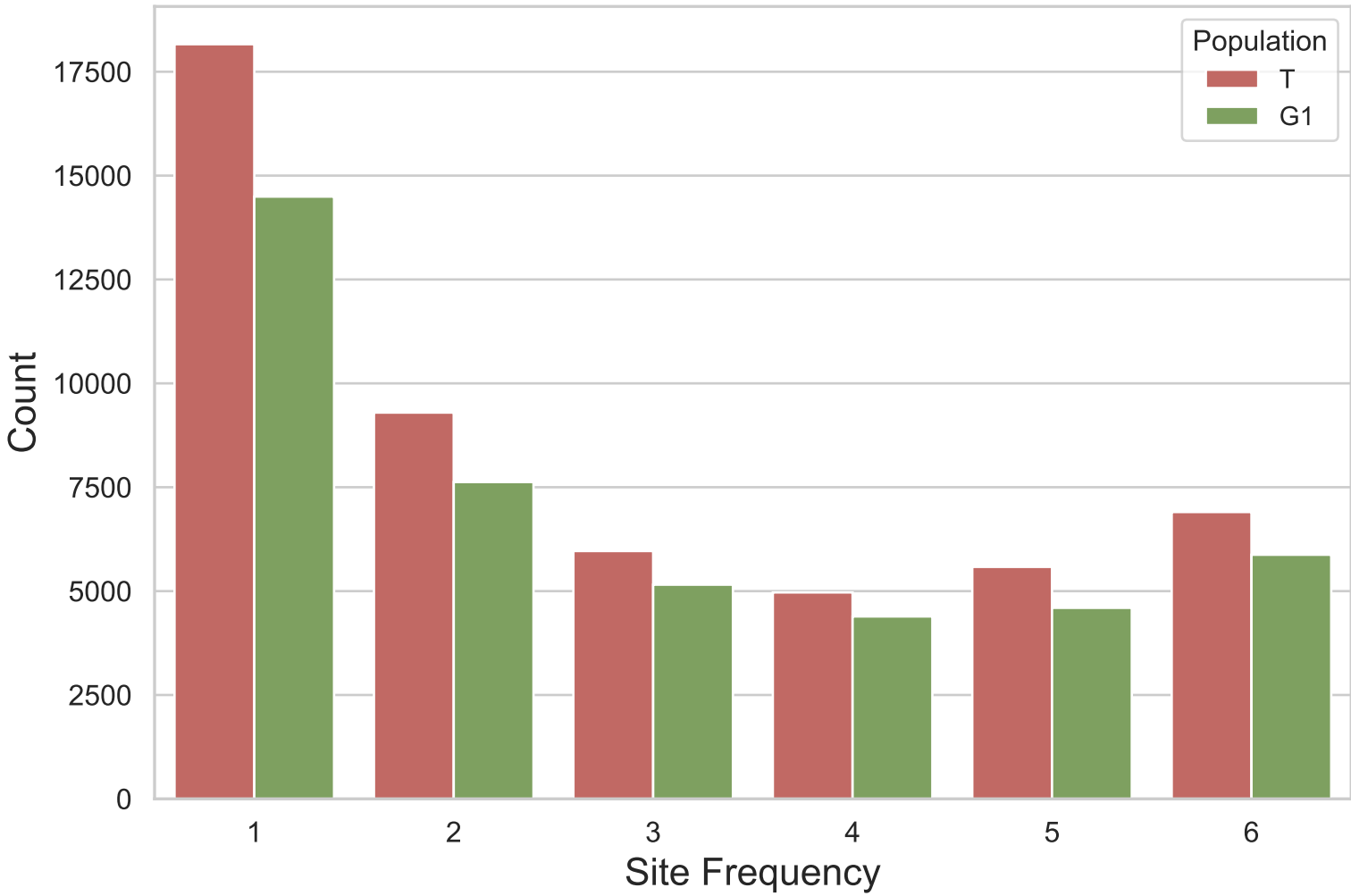
Population
T
G1
17500
15000
12500
10000
7500
5000
2500
0
Count
1
2
3
4
5
6
Site Frequency

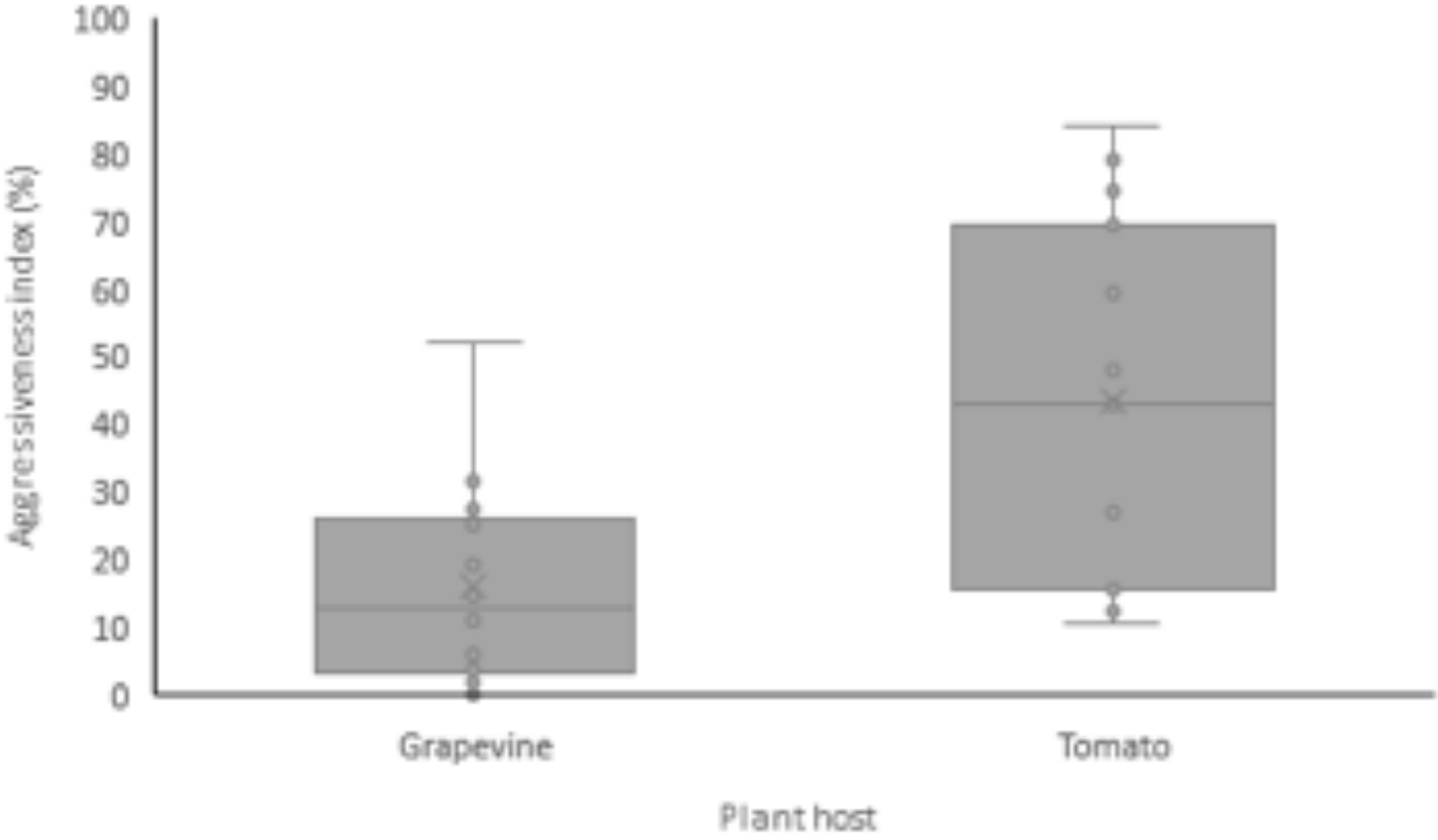
100
90
80
70
60
50
40
30
20
10
0
Aggressiveness index (%)
Grapevine
Tomato
Plant host

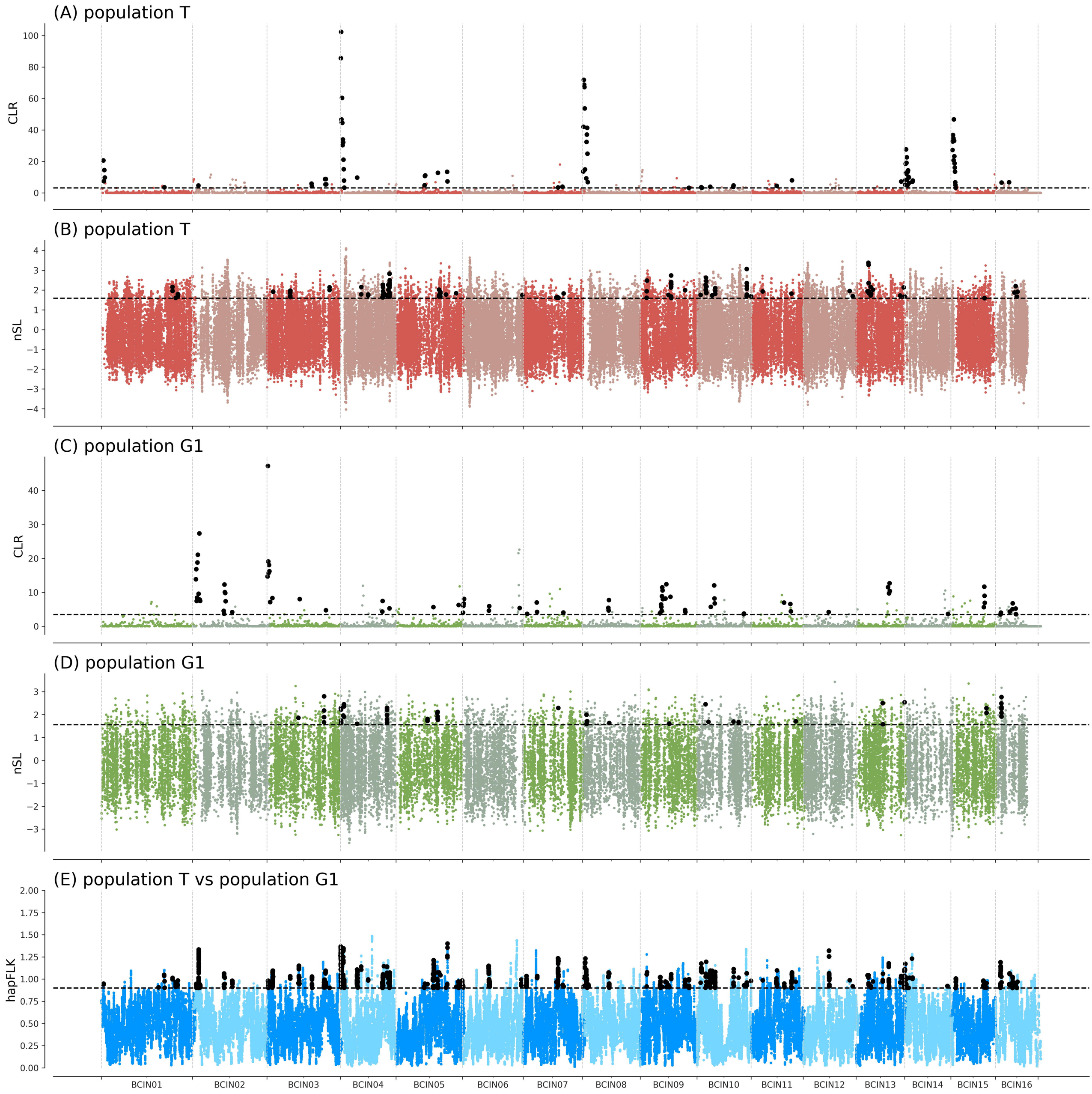
(A) population T
CLR
(B) population T
nSL
(C) population G1
CLR
(D) population G1
nSL
(E) population T vs population G1
hapFLK
BCIN01
BCIN02
BCIN03
BCIN04
BCIN05
BCIN06
BCIN07
BCIN08
BCIN09
BCIN10
BCIN11
BCIN12
BCIN13
BCIN14
BCIN15
BCIN16